MITSUBISHI ELECTRIC RESEARCH LABORATORIES
http://www.merl.com

Narrowband Interference Resilient Receiver Design for Unknown UWB Signal Detection

Onur Ozdemir, Zafer Sahinoglu, Jin Zhang

TR2008-022 June 2008

Abstract

In this article, we design a novel energy-detection based receiver architecture to detect UWB signals in a strong narrowband interference (NBI) environment. Designed receiver is capable of suppressing NBI at low cost without any need for searching its frequency location. This is made possible by preprocessing the received signal using a cascaded nonlinear energy operator followed by a high-pass filter before regular energy detection.

ICC 2008 (May)

Narrowband Interference Resilient Receiver Design for Unknown UWB Signal Detection

Onur Ozdemir, *Student Member, IEEE,* Zafer Sahinoglu, *Member, IEEE,*
Jinyun Zhang, *Senior Member, IEEE*

***Abstract*—In this article, we design a novel energy-detection based receiver architecture to detect UWB signals in a strong narrowband interference (NBI) environment. Designed receiver is capable of suppressing NBI at low cost without any need for searching its frequency location. This is made possible by preprocessing the received signal using a cascaded nonlinear energy operator followed by a high-pass filter before regular energy detection.**

***Index Terms*—Teager-Kaiser, energy detection**

I. Introduction

UWB signaling, in which an extremely wide frequency bandwidth of more than 500 MHz is employed, is an attractive solution for target sensing systems as well as wireless communications. In a sensing system point of view, UWB can provide more information capacity compared to a narrowband system since it utilizes a much wider bandwidth. Particularly, higher target and range resolution can be obtained using an UWB sensing system. As far as the wireless communications is considered, UWB is an attractive solution because it allows for higher data rates at low cost.

One of the key challenging issues regarding UWB transmission systems is the performance degradation due to high-power narrowband signals existing in the environment. Since UWB systems operate over extremely wide frequency bands, they have to co-exist with other narrowband systems which may operate with much higher power levels. In addition, intentional interferers may exist in the environment where they use high power narrowband signals to jam UWB sensing systems. Even though narrowband interferers operate on a very small fraction of the bandwidth utilized by UWB systems, they can completely jam UWB signals because of their relatively high operating power. Therefore, it is necessary to design efficient transceivers that are robust to NBI. Existing techniques dealing with NBI issues consist of two groups which are NBI avoidance techniques employed at the transmitter and NBI cancelation or suppression techniques employed at the receiver. Although many methodologies to cope with NBI have been developed in the literature, none of them has proven to give an optimum solution and they all have severe limitations for UWB systems [1]. Most of the feasible NBI avoidance techniques, such as multiband schemes, multicarrier approaches and pulse shaping methods, require accurate information about the center frequency of the NBI which is not known *a priori* in most of the situations and needs to be estimated. Although many digital NBI cancelation techniques have been developed for wideband systems [2], none of these approaches is practical for UWB systems because of the required extremely high sampling rates and larger dynamic ranges of analog-to-digital converters (ADCs) to resolve NBI. These techniques are mostly based on employing adaptive filters, which behave similar to notch filters, to adaptively estimate and eliminate NBI in digital domain. Analog notch filtering can be an effective approach for canceling NBI in UWB systems, however it is not very efficient since it requires exact information about the NBI to be effective (center frequency, power, etc.) and that the NBI is fixed and always exists [1]. Another method is to use bank of analog notch filters at the receiver which results in high-cost and complex receivers. The most popular technique so far to suppress NBI is to use rake receivers [3] which are also highly complex and their complexity increases depending on the number of rake fingers employed [1]. Furthermore, NBI may exist as a transient in the system which makes most of the NBI avoidance and cancelation techniques ineffective.

Energy detector (ED) is a low-complexity non-coherent detection architecture well-suited for UWB signals, and it is widely used due to its simplicity and good performance. ED does not suffer from the issues related to coherent reception systems such as accurate synchronization, pulse shape estimation and high sampling rates [13]. In an ED scheme, the energy of the received signal is measured and compared to an appropriately selected threshold to determine the presence of a signal. It should also be noted that for an additive white Gaussian noise (AWGN) channel and completely unknown signal parameters, ED provides the uniformly most powerful (UMP) test, i.e. it gives the optimal detection performance [10]. However, if there is an unknown interferer in the system, ED is not UMP anymore and signal energy needs to be increased in order to compensate for the performance degradation caused by the narrowband interference [12].

In this paper, a novel ED based receiver design for UWB systems is developed. Proposed receiver is capable of suppressing NBI in the analog domain at very low additional cost which makes it practical to implement for UWB signal detection. Developed UWB receiver architecture is a generic one in the sense that it can be used in both active and passive sensing systems to detect the presence of targets as well as in wireless communications such as demodulation of on-off keyed (OOK) UWB signals. In the developed receiver architecture, a cascaded nonlinear energy operator and high-pass filter is utilized followed by a classical energy detector. The nonlinear energy operator employed is called the Teager-Kaiser (TK) energy operator [4] which will be explained in Section II. With the help of this energy operator, NBI co-existing with the UWB signal in the system is converted to a low frequency signal and then suppressed using a high-pass filter. Throughout the rest of this article, we will refer to our developed detector as the Teager-Kaiser Energy Detector (TKED).

In Section III, commonly used receiver types are discussed. We introduce our proposed receiver architecture, and analyze the effects of the TK energy operator on different input signal components in Section IV. In Section V, some simulation results are provided to demonstrate the performance of our proposed receiver. Finally, concluding remarks are presented in Section VI.

II. Teager-Kaiser Energy Operator

Teager-Kaiser (TK) energy operator is a nonlinear differential energy operator which was first systematically introduced in [4]-[5], and found some applications in the literature such as transient signal detection [6] and demodulation of AM-FM signals [7]. Let $\psi(s(t))$ denote the continuous time Teager-Kaiser (TK) energy operation on input signal $s(t)$. The $\psi(s(t))$ is defined by

$$\psi(s(t)) = \dot{s}(t)^2 - s(t)\ddot{s}(t) \tag{1}$$

If $s(t) = Acos(2\pi f_c t + \theta)$, then,

$$\psi(s(t)) = A^2(2\pi f_c)^2 \tag{2}$$

It is clear from (2) that the *TK* operator functions as a *frequency-to-DC converter*. The output of the operator is a DC signal which is proportional to the squares of both amplitude and frequency of the sinusoid. To obtain discrete-time representation $s(n)$, assume that $s(t)$ is sampled at frequency f_s. The *TK* energy operator in discrete-time is defined as

$$\psi(s(n)) = s(n)^2 - s(n-1)s(n+1) \tag{3}$$

Note that it is almost an instantaneous operator since it only needs two neighboring samples. If $s(n) = Acos(\Omega n + \theta)$, where $\Omega = 2\pi f_c/f_s$, then,

$$\psi(s(n)) = A^2 sin^2(\Omega) \tag{4}$$

It was also shown in [4] that when $f_s > 8f_c$, $\psi(s(n))$ can be approximated as

$$\psi(s(n)) \approx A^2\Omega^2 \tag{5}$$

III. Commonly Used Receiver Types

It is already well known that matched-filtering, in which the received signal is correlated with a stored signal template at the receiver, provides optimal detection performance when the signal waveform is completely known and background noise is AWGN [9]. The receiver architecture for matched-filtering is shown in Fig.1(a). It is also referred to as the correlation receiver. However, if the noise is gaussian but not white (may be narrowband) and its power spectral density (PSD) is not known, the correlation receiver has to be much more complex in order to estimate the power spectral density of the noise and to use a prewhitening filter before matched-filtering operation. Moreover, if the noise is not gaussian such as a sinusoidal interference, nonlinear receiver architectures that perform maximum-likelihood formulation need to be implemented to obtain optimal performance which are also highly complex and do not have any general structure [9]. Furthermore, if the there is a transient narrowband interference in the system with unknown parameters, none of these approaches are applicable. Even if there is perfect knowledge about the noise in the system, in order to obtain perfect alignment of the received waveform with the template, received signal must be sampled at Nyquist rates and sampling at these high rates may not be always feasible or possible for UWB signals because of their extremely wide bandwidths [14]. In addition, received waveform shape must be perfectly known for the matched-filter to give optimum performance. In UWB sensing systems where the presence of a target is determined by detecting the presence of a reflected signal from the target, the waveform of the reflected signal is completely different than that of the transmitted signal due to many reasons inherent in UWB signals [8]. Therefore matched-filtering is not realizable for an UWB sensing system. Throughout our analysis, we assume that there is no *a priori* information about the interference that may exist in the system and matched-filter in Fig.1(a) will only serve as the standard benchmark case for comparison purposes assuming the only background noise is AWGN and the unknown signal waveform is known.

Fig.1(b) depicts a classical ED in which the received band-pass signal is preprocessed by a low-noise amplifier (LNA) and a band-pass filter (BPF) to reduce the effects of noise. Then the energy of the preprocessed signal is collected via a square-law device followed by an integrator. This scheme enables sampling at sub-Nyquist rates without any significant loss in the performance. However, it should be noted that sampling at lower rates introduces a trade-off between receiver complexity and target/range resolution in a target detection scenario.

In an energy detection problem, the energy measure of the received signal is obtained as follows:

$$y(t) = \frac{1}{\tau}\int_{t-\tau}^{t} |r(t)|^2 dt \tag{6}$$

where $r(t)$ and τ denote the received signal and integration window length respectively. Note that the expression in (6) corresponds to the received signal energy normalized to window length. $y(t)$ in (6) is then sampled with a sampling rate t_s to obtain y_k and compared to a previously defined threshold, γ, to detect the presence of a signal. This problem can be set as a binary hypotheses testing problem in which the interference-plus-noise hypothesis ($\mathcal{H}_0$) is tested against a signal-plus-interference-plus-noise hypothesis ($\mathcal{H}_1$):

$$\begin{aligned} \mathcal{H}_0 &: \quad y_k = i_k + n_k \\ \mathcal{H}_1 &: \quad y_k = s_k + i_k + n_k \end{aligned} \tag{7}$$

where s_k, i_k and n_k denote unknown signal, the interference term and the background noise present in the system. n_k is modeled as white Gaussian noise (WGN) with flat power spectral density σ_n^2, i.e. $n_k \sim \mathcal{N}(0, \sigma_n^2)$. The analysis of ED has been extensively carried out in the literature and the same analysis will not repeated here for brevity. Interested reader should refer to [11]-[14].

IV. Proposed Receiver Architecture

In this section, we design a novel ED based receiver architecture which has a built-in NBI suppression capability for a wideband system. The architecture of the proposed detector is shown in Fig.2. In the proposed architecture, two additional preprocessing blocks which enable to suppress NBI are added

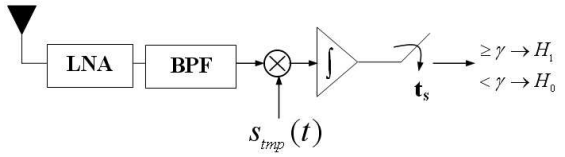

(a) *Matched filter*

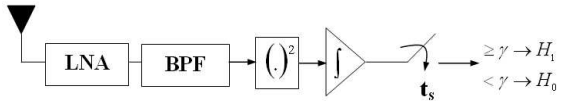

(b) *Energy detector*

Fig. 1. Commonly used receiver architectures for UWB systems

to a classical ED between the BPF and the square-law device. The additional preprocessing blocks are the Teager-Kaiser (TK) energy operator described in Section II and a high-pass filter respectively. The role of the TK operator is to act as a *spectrum-shifter* and move the NBI component of the received signal towards very low frequencies. These low-frequency components resulting from the NBI are then eliminated using a high-pass filter before energy measurement. The mechanism of the TK operator is discussed in the next section.

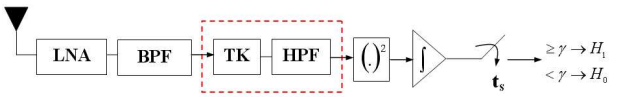

Fig. 2. Proposed receiver design *(TKED)*, dashed lines: additional blocks to an energy-detector

A. Effect of TK Operator on Wideband Signals and NBI

A scenario in which a NBI spectrum overlaps with that of an UWB system is shown in Fig.3.

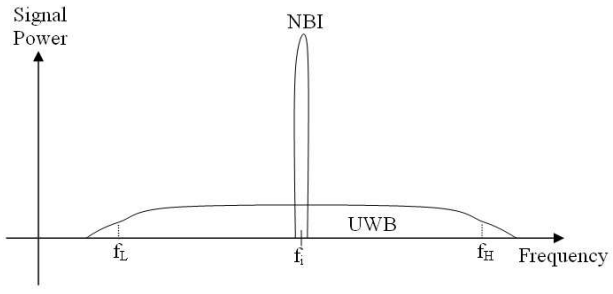

Fig. 3. Overlap between NBI and UWB signal spectrum

NBI can be modeled in two separate ways: 1) single-tone interferer of the form [1]:

$$s(t) = A_i sin(2\pi f_i t + \theta_i) \tag{8}$$

where A_i and f_i are the amplitude and the frequency of the interferer, respectively, or a 2) band-limited interferer whose model is a zero-mean Gaussian random process with power spectral density (PSD) [1]:

$$S_i(f) = \begin{cases} P_i, & f_i - \frac{B_{nbi}}{2} \leq |f| \leq f_i + \frac{B_{nbi}}{2} \\ 0, & \text{otherwise.} \end{cases} \tag{9}$$

where B_{nbi} and f_i are the bandwidth and the center frequency of the interferer, respectively, and P_i is the power spectral density.

In our analysis, the narrowband interferer is modeled as a single-tone interferer as in (8) for analytical simplicity. However, the results derived for a single-tone interferer also apply for an interferer which can be modeled as a band-limited random process as in (9). This will be validated by simulations in the following section.

Suppose the input to a TK operator $s(t)$ is composed of two different frequency components, namely $s_1(t)$ and $s_2(t)$. Then if the TK operator defined in (1) is applied on $s(t)$, the output is

$$\psi(s_1 + s_2) = \psi(s_1) + \psi(s_1) + \psi_c(s_1, s_2) \tag{10}$$

where the cross-term $\psi_c(s_1, s_2)$ is defined as

$$\psi_c(s_1, s_2) = 2\dot{s_1}\dot{s_2} - s_1\ddot{s_2} - s_2\ddot{s_1} \tag{11}$$

Proposition 1: If the input signal, $s(t)$, to a TK operator is composed of N sinusoids with different frequencies given by

$$s(t) = \sum_{i=1}^{N} A_i sin(2\pi f_i t), \tag{12}$$

then

$$\psi(s(t)) = K + \sum_{i=1}^{N}\sum_{j>i}^{N} \gamma_i^j cos\big[2\pi(f_i - f_j)t\big] + \gamma_j^i cos\big[2\pi(f_i + f_j)t\big] \tag{13}$$

where

$$\gamma_i^j = A_i A_j (2\pi f_i)(2\pi f_j) + \frac{A_i A_j (2\pi f_i)^2}{2} + \frac{A_i A_j (2\pi f_j)^2}{2}$$
$$\gamma_j^i = A_i A_j (2\pi f_i)(2\pi f_j) - \frac{A_i A_j (2\pi f_i)^2}{2} - \frac{A_i A_j (2\pi f_j)^2}{2}$$

and K is a constant.

Proof: It was previously shown in Section II that if the input signal to a TK energy operator $\psi(.)$ is a pure sinusoid, the output is a *DC* component whose amplitude is proportional to squares of both of its amplitude and frequency as given in (2). Now, consider $N = 2$, i.e. the input signal, $s_1(t)$, consists of two sinusoids

$$s_1(t) = \sum_{i=1}^{2} A_i sin(w_i t + \phi_i) \tag{14}$$

where $w_i = 2\pi f_i$. Without loss of generality, we can assume that $\phi_i = 0$ for all components. Then the output of the TK energy operator, $\psi(s(t))$ after some manipulations is given by

$$\psi(s_1(t)) = A_1^2 w_1^2 + A_2^2 w_2^2 + \big[A_1 A_2 w_1 w_2 + \frac{A_1 A_2 w_1^2}{2} + \frac{A_1 A_2 w_2^2}{2}\big] cos\big[(w_1 - w_2)t\big] + \big[A_1 A_2 w_1 w_2 - \frac{A_1 A_2 w_1^2}{2} - \frac{A_1 A_2 w_2^2}{2}\big] cos\big[(w_1 + w_2)t\big] \tag{15}$$

Note that (15) is consistent with the expression in (13). Now suppose that $s_2(t) = A_3 sin(w_3 t)$ is added to $s_1(t)$ before feeding it to the TK operator, where $w_1 \neq w_2 \neq w_3$. Then using (2) and (15) in (10),

$$\begin{aligned}\psi(s_1(t)+s_2(t)) &= A_1^2 w_1^2 + A_2^2 w_2^2 + A_3^2 w_3^2 \\ &+ \big[A_1A_2w_1w_2 + \frac{A_1A_2w_1^2}{2} + \frac{A_1A_2w_2^2}{2}\big]cos\big[(w_1-w_2)t\big] \\ &+ \big[A_1A_2w_1w_2 - \frac{A_1A_2w_1^2}{2} - \frac{A_1A_2w_2^2}{2}\big]cos\big[(w_1+w_2)t\big] \\ &+ \psi_c(s_1(t), s_2(t))\end{aligned} \tag{16}$$

where $\psi_c(s_1(t), s_2(t))$ can be derived by putting $s_1(t)$ and $s_2(t)$ in (11)

$$\begin{aligned}&\psi_c(s_1(t), s_2(t)) = \\ &\big[A_1A_3w_1w_3 + \frac{A_1A_3w_1^2}{2} + \frac{A_1A_3w_3^2}{2}\big]cos\big[(w_1-w_3)t\big] \\ &+ \big[A_2A_3w_2w_3 + \frac{A_2A_3w_2^2}{2} + \frac{A_2A_3w_3^2}{2}\big]cos\big[(w_2-w_3)t\big] \\ &+ \big[A_1A_3w_1w_3 - \frac{A_1A_3w_1^2}{2} - \frac{A_1A_3w_3^2}{2}\big]cos\big[(w_1+w_3)t\big] \\ &+ \big[A_2A_3w_2w_3 - \frac{A_2A_3w_2^2}{2} - \frac{A_2A_3w_3^2}{2}\big]cos\big[(w_2+w_3)t\big]\end{aligned} \tag{17}$$

It can be seen from (16) and (17) that $\psi(s_1(t)+s_2(t))$ is also consistent with (12). Hence, it is concluded that for an input consisting of $N \geq 1$ sinusoids, the output of the TK operator consists of a *DC* component and sinusoids with difference and sum frequencies of $(N, 2)$ combinations of $f_1, ...f_N$, in which lower frequency terms have more power compared to their higher frequency counterparts. ∎

Proposition 2: If the input to a TK operator is a bandpass signal with a $3dB$ flat spectrum of amplitude A spanning from f_L to f_H and a center frequency $f_c = (f_L + f_H)/2$, such that $f_c \gg (f_H - f_L)$, then the $3dB$ spectrum of the output signal spans from 0 to $(f_H - f_L)$.

Proof: Let $s(t)$ be a baseband signal consisting of N sinusoidal components having the same amplitude $2A$ with frequencies $f_1 < f_2 < ... < f_N$. Now, suppose that $s(t)$ is modulated with a carrier of frequency f_c, such that $f_c \gg 2f_N$. Then the bandpass signal is given by

$$s_b(t) = \sum_{i=1}^{N} 2A sin(2\pi f_i t + \phi_i) cos(2\pi f_c t). \tag{18}$$

Note that $s_b(t)$ has a bandwidth of $2f_N$ centered at f_c. We can again assume that $\phi_i = 0$ for all components without loss of generality. After some manipulations, $s_b(t)$ can be written as

$$\begin{aligned}s_b(t) &= \sum_{i=1}^{N} A\big[sin\big(2\pi(f_c+f_i)t\big) + \sum_{i=1}^{N}(-A)sin\big(2\pi(f_c-f_i)t\big)\big] \\ &= s_R(t) + s_L(t).\end{aligned} \tag{19}$$

Now, suppose $s_b(t)$ is the input to a TK operator. Then the output is from (10)

$$\psi(s_b(t)) = \psi(s_R(t)) + \psi(s_L(t)) + \psi_c(s_R(t), s_L(t)) \tag{20}$$

As it is observed from (20), $\psi(s_b(t))$ has three terms. Now, each of these terms will be analyzed separately to complete the proof.

From (13), $\psi(s_R(t))$ can be written as

$$\begin{aligned}\psi(s_R(t)) = K_R &+ \sum_{i=1}^{N}\sum_{j>i}^{N} \gamma_i^j cos\big[(w_i - w_j)t\big] \\ &+ \gamma_j^i cos\big[(2w_c + w_i + w_j)t\big]\end{aligned} \tag{21}$$

where

$$\begin{aligned}\gamma_i^j &= A^2(w_c+w_i)(w_c+w_j) + \frac{A^2(w_c+w_i)^2}{2} + \frac{A^2(w_c+w_j)^2}{2} \\ \gamma_j^i &= A^2(w_c+w_i)(w_c+w_j) - \frac{A^2(w_c+w_i)^2}{2} - \frac{A^2(w_c+w_j)^2}{2}\end{aligned} \tag{22}$$

in which $w_i = 2\pi f_i$. Since $f_1 < f_2 < ... < f_N$ and $\frac{f_c}{f_N} \gg 2$, asymptotic expressions can be found in the limit $\frac{f_c}{f_N} \to \infty$ as follows

$$\begin{aligned}\lim_{\frac{f_c}{f_N}\to\infty} \gamma_i^j &= A^2 w_c^2 (2 + \frac{2w_i}{w_c} + \frac{2w_j}{w_c} + \frac{w_i w_j}{w_c^2} + \frac{w_i^2}{2w_c^2} + \frac{w_j^2}{2w_c^2}) \\ &\approx 2A^2 w_c^2\end{aligned} \tag{23}$$

$$\begin{aligned}\lim_{\frac{f_c}{f_N}\to\infty} \gamma_j^i &= A^2 w_c^2 (\frac{w_i w_j}{w_c^2} - \frac{w_i^2}{2w_c^2} - \frac{w_j^2}{2w_c^2}) \\ &\approx 0\end{aligned} \tag{24}$$

Therefore,

$$\lim_{\frac{f_c}{f_N}\to\infty} \psi(s_R(t)) \approx K_R + \sum_{i=1}^{N}\sum_{j>i}^{N} 2A^2 w_c^2 cos\big[(w_i - w_j)t\big] \tag{25}$$

An asymptotic expression for $\psi(s_L(t))$ can also be found by using the same previous analysis.

$$\lim_{\frac{f_c}{f_N}\to\infty} \psi(s_L(t)) \approx K_L + \sum_{i=1}^{N}\sum_{j>i}^{N} 2A^2 w_c^2 cos\big[(w_i - w_j)t\big] \tag{26}$$

The third term $\psi_c(s_R(t), s_L(t))$ can be derived by putting $s_R(t)$ and $s_L(t)$ in (11). Here, we skip some derivation steps for brevity and give the final result:

$$\begin{aligned}\psi_c(s_R(t), s_L(t)) = &\sum_{i=1}^{N}\sum_{j=1}^{N} C_i^j cos\big[(w_i + w_j)t\big] \\ &+ C_j^i cos\big[(2w_c + w_i - w_j)t\big]\end{aligned} \tag{27}$$

where

$$\begin{aligned}C_i^j &= -A^2 w_c^2 (2 + \frac{2w_i}{w_c} - \frac{2w_j}{w_c} - \frac{w_i w_j}{w_c^2} + \frac{w_i^2}{w_c^2} + \frac{w_j^2}{w_c^2}) \\ C_j^i &= A^2(w_i w_j + \frac{w_i^2}{2} + \frac{w_j^2}{2})\end{aligned} \tag{28}$$

Again, taking the limit as $\frac{f_c}{f_N} \to \infty$, $\psi_c(s_R(t), s_L(t))$ can be approximated as follows

$$\begin{aligned}\lim_{\frac{f_c}{f_N}\to\infty} \psi_c(s_R(t), s_L(t)) \approx &\sum_{i=1}^{N}\sum_{j=1}^{N}(-2A^2 w_c^2) cos\big[(w_i + w_j)t\big] \\ &+ \big[\frac{A^2}{2}\big(w_i + w_j\big)^2\big] cos\big[(2w_c + w_i - w_j)t\big]\end{aligned} \tag{29}$$

Note that if $f_c \gg 2f_N$, then $2w_c^2 \gg \frac{(w_i+w_j)^2}{2}$ for all i, j. Therefore the second term in (29) can be neglected resulting in

$$\lim_{\frac{f_c}{f_N}\to\infty} \psi_c(s_R(t), s_L(t)) \approx \sum_{i=1}^{N}\sum_{j=1}^{N}(-2A^2w_c^2)cos\big[(w_i+w_j)t\big]. \tag{30}$$

Finally, collecting the terms in (25), (26) and (30), an approximate asymptotic expression for $\psi(s_b(t))$ can be found

$$\begin{aligned}\psi(s_b(t)) \approx & D + \sum_{i=1}^{N}\sum_{j>i}^{N} 4A^2w_c^2cos\big[(w_i-w_j)t\big] \\ & - \sum_{i=1}^{N}\sum_{j=1}^{N} 2A^2w_c^2cos\big[(w_i+w_j)t\big]\end{aligned} \tag{31}$$

It is clear from (31) that the spectrum of $\psi(s_b(t))$ spans from 0 to $2f_N$. An arbitrary baseband signal with a highest $3dB$ frequency component $f_N = (f_H - f_L)/2$ can be approximated as a sum of N sinusoids with frequencies $0 \le f_1 < f_2 < ... < f_N$ that have a separation Δf in the limit $\lim_{\Delta f\to 0}$. Hence, it is concluded from the above analysis that the corresponding output bandpass signal from the TK operator will span from 0 to $f_H - f_L$ as long as the center frequency $f_c \gg (f_H - f_L)$. ■

The result from *Proposition 2* can be exploited to suppress NBI regardless of its frequency location in a bandpass UWB system. Since the bandwidth of a narrowband interferer is very small compared to the center frequency of an UWB system, any arbitrary NBI in the system will only have low-frequency components after the TK operation. These components can then be eliminated by using a HPF.

Proposition 3: For a physical bandpass transmission system, if there exists a strong NBI in the environment, such that NBI power is much higher than both the corresponding transmission signal and the background noise, and that it is modeled as a single-tone interferer, then TKED strictly outperforms ED.

Proof: Consider a scenario in which there is only one single-tone interferer with frequency f_1

$$i(t) = A_1 sin(2\pi f_1 t). \tag{32}$$

Let the unknown bandpass signal to $s(t)$ to have unity power and be the sum of two sinusoids with frequencies f_1 and f_2 without loss of generality.

$$s(t) = sin(2\pi f_1 t) + sin(2\pi f_2 t). \tag{33}$$

Consider the case when $\mathcal{H}_1$ is true, i.e. the unknown signal is present in the received signal:

$$r(t) = s(t) + i(t) + n(t) \tag{34}$$

in which $n(t)$ denotes the background WGN. We assume that NBI is the dominant noise in the system and it has much higher relative power compared to the WGN as well as the unknown signal (i.e. $A_1 \gg 1, \sigma^2$), which is usually the case in an UWB transmission systems when there is strong NBI in the environment. With these assumptions, the received signal can be approximated as

$$r(t) \approx A_1 sin(2\pi f_1 t) + sin(2\pi f_2 t). \tag{35}$$

$r(t)$ is first passed through a LNA followed by a BPF as in the classical ED and then fed into a TK energy operator. The output of the TK operator is the same as (15) except that $A_2 = 1$ in this case.

In order to compare the performances of ED and TKED under strong NBI, a measure called *deflection coefficient* [9] can be utilized. The *deflection coefficient* for a binary detection problem in which the variance is identical for both hypotheses is defined as

$$d^2 = \frac{\big(E(T;\mathcal{H}_1) - E(T;\mathcal{H}_0)\big)^2}{var(T;\mathcal{H}_0)} \tag{36}$$

where T denotes the test statistics and $E(.)$ is the expectation operator. It is easy to see from (36) that d^2 is the ratio of the distance between the expected values to the variance of the test statistics provided that the variance is the same under both hypotheses. Detection performance increases with increasing d^2. Let T_{ED} and T_{TKED} denote the test statistics of ED and TKED respectively. For a strong NBI, it can easily be shown that

$$\begin{aligned}\lim_{A_1\to\infty} & var(T_{ED};\mathcal{H}_0) \approx var(T_{ED};\mathcal{H}_1) \\ & \approx var(T_{TKED};\mathcal{H}_0) \approx var(T_{TKED};\mathcal{H}_0) \approx 0\end{aligned} \tag{37}$$

Therefore the the performances of ED and TKED in a strong NBI environment can be compared by just comparing the distance between the expected values of test statistics under both hypotheses. Greater the distance, better the detection performance. For this purpose, another measure can be defined as follows:

$$\eta^2 = \big(E(T;\mathcal{H}_1) - E(T;\mathcal{H}_0)\big)^2. \tag{38}$$

Detection performance increases with increasing η^2. Now suppose that a simple *DC-Removal* circuitry is used as a HPF in TKED (Fig. 2), and the window length is predefined such that $\tau = N_1 2\pi f_1 = N_2 2\pi f_2$ where N_1 and N_2 are integers. Let η^2_{ED} and η^2_{TKED} denote the performance measures for ED and TKED respectively. Then for a strong single-tone NBI, using the signal models in (32) and (35), η^2 for both detectors can be obtained after some calculation as

$$\eta^2_{ED} \approx \frac{1}{2} \tag{39}$$

$$\eta^2_{TKED} \approx \frac{3}{2}A_1^2w_1^2w_2^2 + \frac{1}{4}A_1^2w_1^4 + \frac{1}{4}A_1^2w_2^4 \tag{40}$$

where $w_1 = 2\pi f_1$ and $w_2 = 2\pi f_2$. Note that the assumption, $(A_1+1) \approx A_1$, made in (35) is incorporated in (40), where all the terms include the coefficient A_1 which is the amplitude of NBI. However, it should be kept in mind that (40) is only an approximation for $A_1 \gg 1$ and η^2_{TKED} will still be nonzero when there is no NBI in the system. It can easily be seen from (39) and (40) that η^2_{TKED} is strictly greater than η^2_{ED} for physical bandpass scenarios considered throughout this work. In fact, η^2_{TKED} can be made smaller than η^2_{ED} only for a very small subspace of w_1 and w_2 which is impossible to exist in physical bandpass systems. Therefore, the designed detector (*TKED*) is expected to give improved performance at all times compared to a classical energy detector (*ED*) when there is a strong narrowband interferer in the environment. ■

For the NBI to degrade the UWB detector performance significantly, NBI must have a very high relative power compared

to the UWB signal do be detected. In conclusion, the added preprocessing blocks, *TK* and *HPF* in Fig. 2, act as a NBI suppresser, or in other words as a wideband signal enhancer. Although the signal models considered throughout this section are not UWB, it is simpler to analytically derive the TK effect on NBI using these signal models since the conclusion holds as long as the unknown signal bandwidth Δf_s is greater than the total bandwidth of narrowband interferers Δf_{nbi}, i.e. $\Delta f_s > \Delta f_{nbi}$. In fact, the performance improvement of TKED over ED increases with increasing $\Delta f_s/\Delta f_{nbi}$ ratio, since the signal energy will be spanned over a wider bandwidth preserving more cross-term components after HPF. This result requires tedious mathematical calculations and it is omitted in this paper. However, the intuition and the methodology is the same as the analysis carried out in (10-40)[1].

B. Effect of TK Operator on AWGN

It was shown in [7] that if the input to a TK energy operator $\psi(.)$ is a zero-mean, stationary Gaussian noise $n(t)$ with autocorrelation $R(\tau)$ and power spectral density $P(w)$, then the output will again be a stationary noise with

$$E\big[\psi(n)\big] = -2R^{(2)}(0) = \frac{1}{\pi}\int_R w^2 P(w)dw \tag{41}$$

$$var\big[\psi(n)\big] = 3\big[R^{(2)}(0)\big]^2 + R(0)R^{(4)}(0). \tag{42}$$

It is seen from (41) and (42) that both moments increase with increasing frequency. Therefore the analysis is frequency-dependant and very tedious. It was also shown in [7] that the predicted performance of the TK operator is highly improved if the signal is pre-filtered using a bandpass filter before feeding it to a TK operator. Note that TK is a highly nonlinear operator and the exact mathematical expressions for the noise statistics after TKED is analytically intractable. However, an intuitive reasoning can be made by considering the BPF employed before the TK operator in Fig. 2 and the results in IV-A. Since the unknown signal bandwidth is known *a priori* and the received signal is pre-filtered using a BPF, the bandwidths occupied by the signal (Δf_s) and the noise (Δf_n) will be almost identical after BPF. Hence, according to the analysis in IV-A, the TK operator will enhance both of them the same amount. Therefore it can be concluded that for the case in which there is only WGN in the system (no NBI), the TKED will not result in any performance loss compared to a classical ED. This conclusion will also be verified by simulations in the next section.

C. System Performance Analysis

The same notation in (7) can be used to analyze the performance of the proposed receiver. Since the main goal is to test the interference-plus-noise hypothesis ($\mathcal{H}_0$) against a signal-plus-interference-plus-noise hypothesis ($\mathcal{H}_1$), it is important to derive the test statistics for both hypotheses. For a given time, let s, i and n denote the unknown wideband signal, the NBI and the Gaussian noise in the system, respectively. Note that the time index is ignored for simplicity without loss of generality. Suppose the NBI is a single-tone interferer with unknown frequency and the HPF used in TKED is a simple *DC-Removal* circuitry. Now, consider the case where $\mathcal{H}_0$ is true, i.e. there is no unknown wideband signal present in the received signal. Then the output of the TK operator is

$$\psi(i+n) = \psi(i) + \psi(n) + \psi_c(i,n) \tag{43}$$

where $\psi(i)$ is the zero-frequency term resulting from single-tone interferer (NBI), $\psi(n)$ is the noise term and $\psi_c(i,n)$ is the $noise + NBI$ cross-term. After passing $\psi(i+n)$ through the HPF, the zero-frequency interference term $\psi(i)$ is totally removed from the system. The remaining high-pass filtered terms are denoted by $\psi(n)_h$ and $\psi_c(i,n)_h$. The final output from the square-law device and the integrator is then

$$y(t) = \frac{1}{\tau}\int_{t-\tau}^{t} |\psi(n)_h + \psi_c(i,n)_h|^2 dt. \tag{44}$$

The same analysis can be carried out for the case where $\mathcal{H}_1$ is true, i.e. the unknown wideband signal is present in the received signal. In this case, the output of the TK operator is

$$\begin{aligned}\psi(s+i+n) = \psi(s) + \psi(i) + \psi(n) \\ + \psi_c(s,i) + \psi_c(s,n) + \psi_c(n,i)\end{aligned} \tag{45}$$

in which $\psi(s)$, $\psi_c(s,i)$ and $\psi_c(s,n)$ are the signal term, the $signal + NBI$ cross-term and the $signal + noise$ cross-term, respectively. Again employing HPF with the remaining components in TKED, the final result can be written as

$$\begin{aligned}y(t) = \frac{1}{\tau}\int_{t-\tau}^{t} |\psi(s)_h + \psi(n)_h + \psi_c(s,i)_h \\ + \psi_c(s,n)_h + \psi_c(n,i)_h|^2 dt\end{aligned} \tag{46}$$

where the subscript *h* denotes the high-pass filtered terms. The probability density functions (pdfs) of the test statistics for $\mathcal{H}_0$ and $\mathcal{H}_1$ hypotheses cannot be derived, therefore the performance is analytically intractable. However, the the results from Sections IV-A and IV-B are enough to justify the superiority of TKED over ED.

V. Simulations

In order to visualize the effects of the proposed receiver blocks in a strong NBI environment, the spectrum of the received signal components are plotted at three different stages of the designed detector (TKED). A modulated raised cosine pulse with a carrier frequency of $2GHz$ and duration $T_p = 16ns$, which has a 3dB bandwidth of 500 MHz, is employed as the unknown UWB signal to be detected. In order to illustrate the generality of our analysis in Section IV-A, NBI is modeled as a narrowband Gaussian process with a bandwidth of 40MHz. Fig. 4 depicts the spectrum of the received signal components for an energy-to-interference-plus-noise ratio (EINR) of $25.4dB$ and interference-to-noise ratio (INR) of $8.1dB$ at three different stages of TKED: 1) input signal to TK in Fig. 4(a), 2) after TK in Fig. 4(b), 3) after HPF in Fig. 4(c). It is clear from Fig. 4(a) and Fig. 4(b) that TK shifts the spectrum of the received signal components towards low frequencies as was discussed in Section IV-A. The input spectrum in Fig. 4(a) spans from $1.75MHz$ to $2.25Mhz$, whereas the output spectrum in Fig. 4(b) ranges from 0 to

[1]Alternatively, the same analysis can also be carried out by using Fourier Transform. However, it is analytically simpler to use real sinusoids in order to visualize and prove the main intuition.

$500MHz$ which verifies our analysis in Section IV-A. Fig. 4(c) illustrates the effect of the HPF by which most of the NBI component is suppressed.

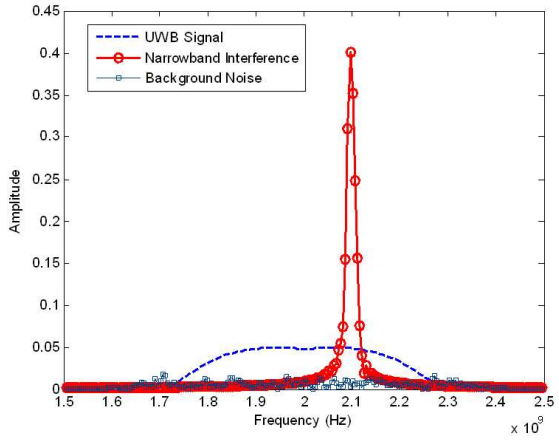

(a) Input Signal

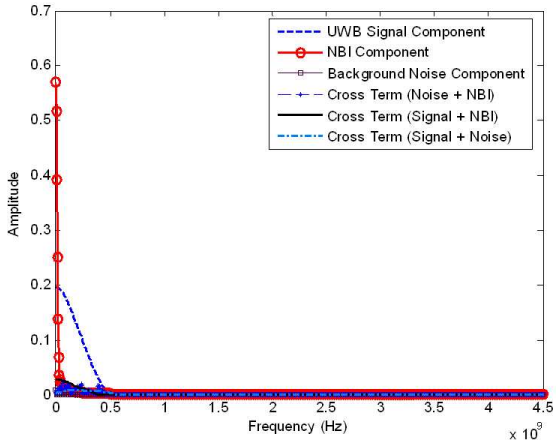

(b) After TK

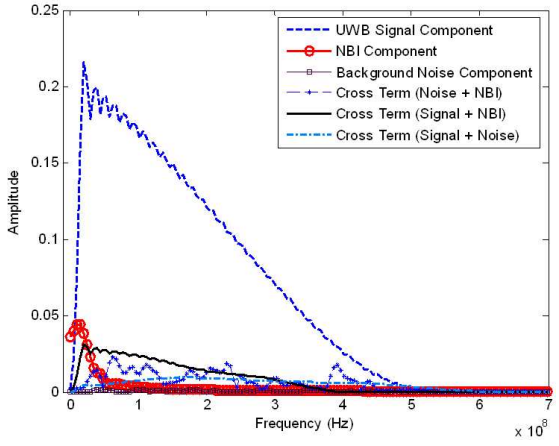

(c) After HPF (Zoomed)

Fig. 4. Spectrum of received signal components in *TKED*

Next, computer simulations are performed to compare the detection performance of the designed receiver with different receiver architectures. Note that the specifications of HPF employed in TKED are design criteria and different types of HPF can be designed depending on the unknown signal bandwidth and NBI, however there is no optimal design since the parameters of NBI that may exist in the system are unknown and can be nonstationary. Here, we employ two different HPFs for comparison purposes. The first one is a simple DC removal circuitry and the second one is a sixth-order Butterworth filter with a $3dB$ cut-off frequency of 30MHz, where the corresponding detectors are called $TKED_1$ and $TKED_2$, respectively. The receiver types compared in the simulations with their abbreviations are described in Table I. As it was discussed before, matched-filter (MF) is considered as the benchmark receiver for comparison purposes. The same modulated raised cosine pulse shown in Fig. 4 is employed as the unknown UWB signal to be detected for all scenarios. Integration window length is set to be equal to pulse duration, i.e. $\tau = T_p = 16ns$. Energy-to-interference-plus-noise ratio (EINR) loss with respect to MF is considered as the performance criteria for a given false-alarm rate (P_{FA}) and probability of detection (P_D). For this reason, P_D curves are plotted for different receivers. The detection thresholds for different detectors for a given P_{FA} are computed numerically based on 10000 Monte-Carlo runs. This is a reasonable method for real physical scenarios when there are no closed-form expressions for the decision statistics, so that the threshold can be defined adaptively by assuming there is no signal present for a certain amount of time length. After the threshold selection, 1000 Monte-Carlo simulations are performed for each $EINR$ to find the corresponding P_D.

TABLE I
COMPARED RECEIVER TYPES

Abbreviation	Receiver Description
ED	Energy detector
TK + ED	Proposed detector with no HPF
TK + DC Removal + ED	$TKED_1$
TK + Butterworth HPF + ED	$TKED_2$
MF	Matched filter

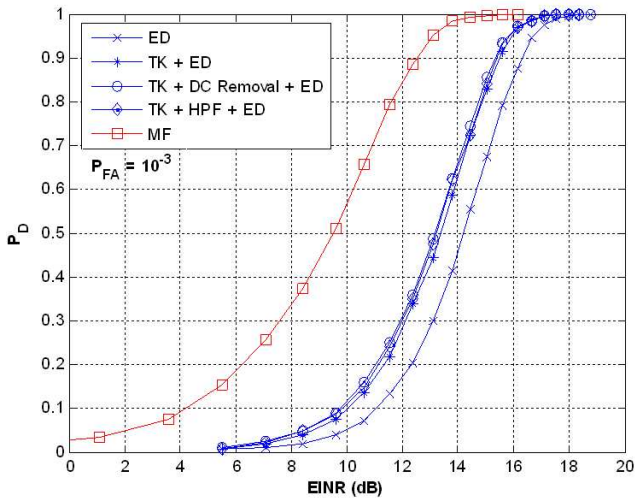

Fig. 5. No NBI present in the system ($INR = -\infty$ dB)

In Fig. 5, performance of different detectors are compared for a given P_{FA} of 10^{-3} when there is no NBI present in the system, i.e. background noise is the only performance degrader. As it is clearly seen from the figure, even when there is only background noise in the system, TKED improves

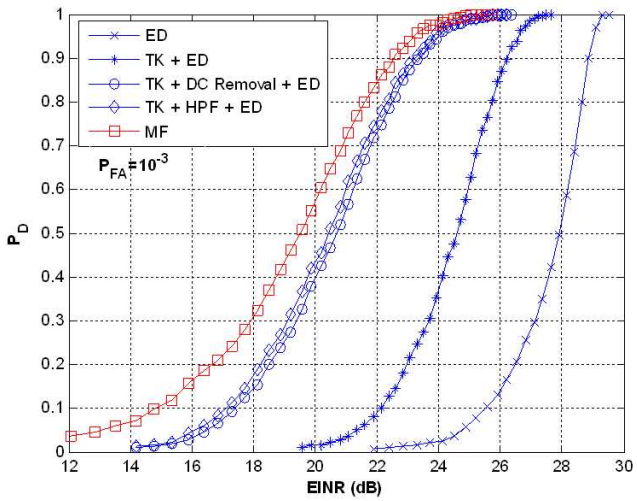

Fig. 6. Strong NBI present in the system ($INR = 7.55dB$)

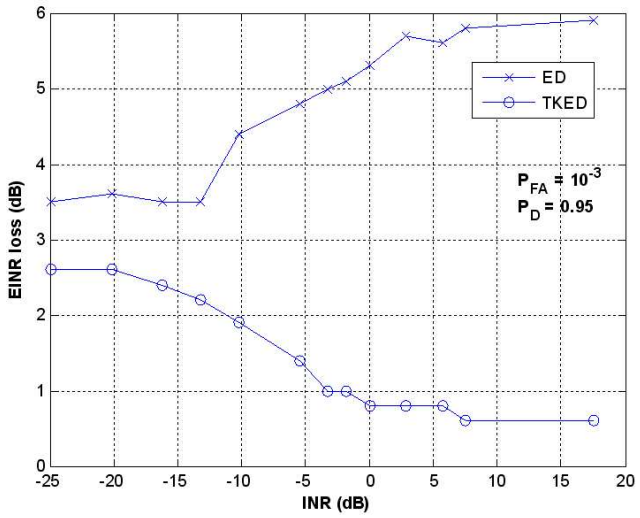

Fig. 7. *EINR* loss with respect to *MF*

the performance over ED by $\sim 0.7dB$ for a $P_D = 0.95$. This slight improvement is the result of $signal + NBI$ and $signal + noise$ cross-terms adding positively to the signal energy, i.e. test statistics under $\mathcal{H}_1$. These results verify the discussion in Section IV-B, i.e. TK has the same effect on wideband noise as on the UWB signal. Note also that using a HPF has no effect on the performance since there is no NBI in the system.

Fig. 6 compares the detection performance of detectors under a strong NBI condition. In this scenario, there is still background noise whose power is the same as in Fig. 5 in addition to the strong NBI (Fig. 4). Note that $INR = 7.55dB$, which indicates that NBI is the dominant performance degrader in the system. In this case, for a $P_D = 0.95$, performance improvement of TK over ED is much significant ($\sim 3.5dB$) and this improvement does even get better ($\sim 5dB$) when a HPF is incorporated, where the performance is almost identical to that of MF, i.e. $EINR$ loss with respect to MF is only $\sim 0.5dB$. This is the performance improvement obtained by our proposed detector architecture, *TKED* shown in Fig. 2.

Finally, Fig. 7 compares the $EINR$ losses of ED and TKED with respect to MF, for increasing NBI power (*INR*), given $P_{FA} = 10^{-3}$ and $P_D = 0.95$. It is clear from Fig. 7 that the performance of the designed detector (TKED) approaches to that of the MF under strong NBI environment as expected, whereas the performance of the classical ED degrades with increasing INR.

VI. Conclusion

In this work, we have designed a novel ED based receiver, which we refer to as *TKED*, for UWB systems that is capable of suppressing NBI regardless of its frequency location. This is made possible at low-cost by incorporating two additional preprocessing blocks to a classical ED. These preprocessing blocks are easy to implement and can be implemented in analog domain resulting in a practical and cost-effective receiver architecture. By implementing *TKED* as an UWB signal receiver, the need for existing complex NBI suppression techniques such as frequency estimation and notch filtering are eliminated without sacrificing any detection performance.

Acknowledgment

The authors would like to thank Dr. A. F. Molisch and Dr. K. H. Teo for useful discussions throughout this work.

References

[1] H. Arslan, Z. N. Chen, M. G. Di Benedetto, Ultra-wideband Wireless Communication. Hoboken, NJ: John Wiley & Sons, 2006.
[2] L. B. Milstein, Interference rejection techniques in spread spectrum communications, Proceedings of the IEEE, vol. 76, no. 6, pp.657-671, June 1988.
[3] I. Bergel, E. Fishler, H. Messer, Narrow-band interference suppression in time-hopping impulse-radio systems, IEEE Conf. on Ultra Wideband Syst. Technol., pp.303-307, May 2002.
[4] J. F. Kaiser, On a simple algorithm to calculate the 'energy' of a signal, IEEE International Conference on Acoustics, Speech and Signal Processing, vol. 1 , pp.381-384, April 1990.
[5] J. F. Kaiser, Some useful properties of Teager's energy operators, International Conference on Acoustics, Speech and Signal Processing, vol. 3 , pp.149-152, April 1993.
[6] R. B. Dunn, T. F. Quatieri, J. F. Kaiser, Detection of transient signals using the energy operator, International Conference on Acoustics, Speech and Signal Processing, vol. 3, pp. 145-148, April 1993.
[7] A. C. Bovik, P. Maragos, T. F. Quatieri, Measuring amplitude and frequency modulations in noise using multiband operators, IEEE-SP International Symposium on Time-Frequency and Time-Scale Analysis, pp. 3-6, Oct. 1992.
[8] J. D. Taylor, Ultra-wideband Radar Technology. Boca Raton, FL: CRC Press LLC, 2001.
[9] S. M. Kay, Fundamentals of Statistical Signal Processing, Vol:II - Detection Theory. Upper Saddle River, NJ: Prentice Hall, 1998.
[10] S. Gezici, Z. Sahinoglu, V. Poor, On the optimality of equal gain combining for energy detection of unknown signals, IEEE Communication Letters, vol. 10, no. 11, pp.772-774, November 2006.
[11] H. Urkowitz, Energy detection of unknown deterministic signals, Proc. of IEEE, vol. 55, no. 4, pp.523-531, April 1967.
[12] E. D. Banta, Energy detection of unknown deterministic signals in the presence of jamming, IEEE Trans. Aerospace and Electronic Systems, vol. 14, no. 2, pp.523-531, March 1978.
[13] M. E. Sahin, I. Guvenc, H. Arslan, Optimization of Energy Detector Receivers for UWB Systems, IEEE 61st Vehicular Technology Conference, vol. 3, pp.1386-1390, May 2005.
[14] I. Guvenc, Z. Sahinoglu, P. Orlik, TOA estimation for IR-UWB systems with different transceiver types, IEEE Trans. Microwave Theory and Techniques, vol. 54, no. 4, pp.1876-1886, June 2006.